DE GRUYTER Main Group Met. Chem. 2019; 42: 81–93

Research Article **Open Access**

Run-Ning Zhao*, Rui Chen, Fan Lin and Zhen-Wu Sun

The stabilities and geometries of Re-encapsulated Si_n(n=16, 20, 24, 28, 32, 36, and 40) clusters: A computational investigation

https://doi.org/10.1515/mgmc-2019-0009
Received October 04, 2018; accepted February 03, 2019.

Abstract: Geometry optimization of the mixed Si_nRe (n=12, 16, 20, 24, 28, 32, 36, and 40) cages with doublet, quartet, and sextet spin configurations is carried out systematically at the UHF/LanL2DZ level. Equilibrium structures, total energies, and stabilities of Re@Si_n cages are presented and discussed. The calculated results show that all Re@Si_n cages of highest symmetry undergo slight distortion into much more stable structures of lower symmetry. The Re atom in the Re@Si_n (n=12, 16, 20, 24, 28, 32, 36, and 40) cages deviates from the cage center site of Si_n fullerenes. Charge-transfer between Re and Si atoms makes a contribution to the stability of the Si_n fullerenes; In addition, the relative stability is discussed, the most stable geometry is assigned.

Keywords: ab initio calculation; stabilities; geometries; cages; transition metal

1 Introduction

There is currently great of interest in utilizing small atomic clusters as constituent elements to build up well-controlled nanostructures (Chen et al., 2018; Han and Shi, 2001; Han et al., 2004; Hiura et al., 2001; Guo et al., 2006; Jarrold, 1991; Majumder and Kulshreshtha, 2004; Miyazaki et al., 2002; Piqueras et al., 1993; Turker, 2001a, Turker, 2001b; Wang and Han, 2005a; Wang and Han, 2005b; Xiao et al., 2002; Xu et al., 2010; Yang et al., 2015; Zhao et al., 2016; Zhao et al., 2017a; Zhao et al., 2017b; Zhao et al., 2018). The assembling of small clusters opens the possibility of building materials with novel properties and the clusters have to retain their character in the new nanomaterial. In the other words, the clusters do not lose their identy when they form cluster solids. This is because clusters have a high intrinsic stability, that is, they are magic species. One can expect that the so called magic clusters, with their specially unreactive electronic structure could be good candidates to form the building blocks of new assembled nanomaterials. Furthermore, depending on the size, silicon clusters show optical properties and reactivity, which are different from those of molecules and solids. For these reasons, theoretical and experimental investigations on the atomic clusters of semiconductor elements are currently intense in order to design advanced material having desired electronic and optical properties (Shvartsburg et al., 2000; Zhao et al., 2018). Among these studies, the small and intermediate-size clusters have received a great deal of attention because of their technological applications in microelectronic industry and their importance in understanding the bright photoluminescence properties found in porous silicon.

It is known that pure silicon clusters are unsuitable as the building blocks and chemically reactive due to the existence of dangling bonds, Interestingly, transition metal(TM) atoms due to their flexibility and variability of valence shell configurations (Zhao et al., 2017a) and the large range of possible bonding patterns can saturate the dangling bonds of Si frame and stabilize Si frame and have enhanced chemical stabilities because of large highest occupied orbital (HOMO) and lowest unoccupied orbital (LUMO) gaps in the most stable geometries with closed-shell electronic structures of extraordinary stabilities and interesting properties (Zhao et al., 2016; Zhao et al., 2017b). The distinct semiconducting and metallic characters of the TM@Si_n clusters lead to a new field of silicon-based nanoscale applications in developing miniature and optoelectronic devices.

---

* **Corresponding author: Run-Ning Zhao,** Institute of Applied Mathematics and Physics, Shanghai DianJi University, Shanghai 201306, People's Republic of China; National Synchrotron Radiation Laboratory, University of Science and Technology of China, Hefei 230029, People's Republic of China, e-mail: zhaorunning@126.com.
Rui Chen, Fan Lin and Zhen-Wu Sun, Institute of Applied Mathematics and Physics, Shanghai DianJi University, Shanghai 201306, People's Republic of China.

A series of experimental results indicate that the endohedral or exhohedral transition metal atoms on small C_{28}, $C_{36,}$ and C_{60} clusters (Buehl and Hirsch, 2001; Chen et al., 2018; Turker, 2001a; Turker, 2001b; Wang and Han, 2005a) can dramatically increase the cluster's stability. Moreover, the photoelectron spectra of the TM-doped silicon cluster anions were observed experimentally (Xu et al., 2010). These findings lead to the theoretical investigations on the Pt_2Si_{16}, $PdSi_{60}$, MSi_{28}, and $ZrSi_{20}$ systems (Han et al., 2002; Jarrold, 1991; Jackson and Nellermoe, 1996; Turker, 2001a; Turker, 2001b; Zhao et al., 2016; Zhao et al., 2017a; Zhao et al., 2017b). To our knowledge, no theoretical investigation on the Re@Si_n (n=12, 14, 16, 20, 24, 28, 32, 36, and 40) fullerenes is reported up to now. In order to give a prediction of experimental results and give a reasonable explanation of the experimental phenomenon, we have carried out the computational studies of total energies and the possible geometries of the Re@Si_n (n=12, 14, 16, 20, 24, 28, 32, 36, and 40) fullerenes.

2 Results and discussions

On the basis of the calculated results on the transition metal doped Si_n clusters, it indicates that the mixed transitional metal silicides are in favorable of forming endohedral cagelike structures which depend strongly upon the transition metal atom and the size of the Si_n clusters (Guo et al., 2006; Han and Shi, 2001; Han, 2003; Han and Hagelberg, 2009; Wang and Han, 2006; Wu and Hagelberg, 2009). Previous theoretical investigations on the $ReSi_n$(n=1-12) clusters indicate that the Re atom localizes at the center site of the Si_n frames when the size of the $ReSi_n$ clusters is bigger than 8 (Han and Shi, 2001), therefore, only the Re-encapsulated Si_n cages are considered in the following sections.

2.1 $ReSi_{12}$

The $ReSi_{12}$ isomers under well-defined D_{6h} and D_{4h} symmetries with different spin states considered are optimized at the UHF/LanL2DZ level. The possible D_{6h} $ReSi_{12}$ isomer is preferentially considered as the ground state candidate. The doublet D_{6h} isomer is optimized to be the stable structure. The calculated Si(6)-Si(12) distance and Si(5)-Si(6) bond length at the UHF/LanL2DZ level are slightly shorter as compared to those at the B3LYP/LanL2DZ level (Han and Shi, 2001). Furthermore, the Re-Si(6) bond length of the doublet D_{6h} $ReSi_{12}$ isomer at the UHF/LanL2DZ level being 2.617 Å is slightly shorter than that (2.690 Å) of the D_{6h} isomer at the B3LYP/LanL2DZ level. The electronic state of the D_{6h} isomer is labeled as having $^2B_{2g}$ character. On the basis of the calculated results of the stable $ReSi_{12}$ cage, the sandwichlike $ReSi_{12}$ cage can be seen as the building block of new material. The new distorted D_{4h} isomer is taken into account; the calculated results reveal that the D_{4h} isomer is an unstable isomer. After the D_{4h} symmetry undergoes a slight distortion to the lower symmetry, the equilibrium geometry of the stable doublet C_1 $ReSi_{12}$ isomer is finally obtained. According to the total energies of the C_1 and D_{6h} isomers, it is worthwhile pointing out that the C_1 isomer is 0.589 eV lower in total energy than the D_{6h} isomer, therefore, the C_1 isomer is selected as the ground state. The Re atom is surrounded by all Si atoms, furthermore, the Re atom tries to terminate the dangling bonds of the silicon atoms and has a tendency to obtain more charges from the Si_{12} frame; Thus, the Re atom acts as an acceptor of charge and enhances the stability of the Si_{12} frame.

2.2 $ReSi_{16}$

Equilibrium geometry of the C_1 $ReSi_{16}$ cage is obtained at the UHF/LanL2DZ level (Table 1). The calculated result of the sextet C_1 $ReSi_{16}$ isomer has one imaginary frequency, which corresponds to a transition state. From the calculated total energies of the C_1 isomer with spin S=1/2 and 3/2, it obviously shows that total energies correlate with the spin states, in the other words, the C_1 isomer with S=3/2 is more stable than with spin S=1/2. Mullikan atomic net populations of the Re atom in the C_1 $ReSi_{16}$ isomer with spin S=1/2 and 3/2 are −3.660e and −2.798e, respectively. In light of the calculated Mullken atomic net populations, it apparently indicates that the charges in the doublet isomer transfer mainly from the Si(i) (i=5, 8, 13, 14) atoms to the Re atom, and that the charges in the quartet cage transfer from the Si(i) (i=5, 8, 13) atoms to the Re atom. The electrostatic interactions among the Re and Si atoms of the double isomer arising from charge distribution is stronger than those of the quartet isomer.

On the basis of the optimized geometry, one finds that the Re atom of the new C_s isomer deviates slightly to center site of the Si_{16} frame. Mullikan atomic net populations of the doublet C_s isomer show that the charges transfer from the Si atoms to the Re atom; furthermore, the charge-transfers among the Re and S(i) (i=1-8) atoms are bigger than those among the Re and Si(j) (j=9-16) atoms. The net population of the Re atom is −3.3136e, the obtained charge of Re atom is transferred to the 4d orbitals, reflecting that the electrostatic interactions between the Re atom and

Table 1: Total energies, the shortest Re-Si bond lengths, Mullikan atomic population of the Re atom (Re(M)), electronic state, and the lowest harmonic frequencies of the $ReSi_n$ (n=12, 16, 20, 24, 28, 30, 32, 36, and 40) fullerenes. (Unit: Å for bond length; cm^{-1} for frequency; hartree for total energy).

System	symm	spin	Re-Si	frequencies	electronic state	Re(M)	E_T
$ReSi_8$	Cs	1/2	2.298		$^2A'$	-3.712	-108.1321987
		3/2	2.310		$^4A'$	-4.116	**-108.133719**
		5/2	2.308		$^6A'$	-3.512	-108.1030331
$ReSi_{12}$	D_{6h}	1/2	2.617	107.2	$^2B_{2g}$	-3.726	-123.1021747
	C_1	1/2	2.342	74.6	^2A	-3.687	**-123.123822**
$ReSi_{16}$	C_1	1/2	2.670	60.0		-3.660	-138.1262721
		3/2	2.685	97.0		-2.798	-138.1666145
		5/2	2.701	-50.7		-3.659	-138.1802717
$ReSi_{16}$	C_s	1/2	2.650	88.9	$^2A'$	-3.314	**-138.1864874**
		3/2	2.612	49.0	$^4A'$	-3.438	-138.1701797
		5/2	2.561	164.3	$^6A'$	-3.659	-138.1814594
$ReSi_{20}$	C_1	1/2	2.710	89.7	^2A	-1.764	**-153.1690535**
		3/2	2.744	67.5		-2.145	-153.1444314
		5/2	2.725	69.9		-2.147	-153.1503386
$ReSi_{24}$	C_1	1/2	2.627	80.2	^2A	-1.530	**-168.1729979**
		3/2	2.660	25.4		-0.206	-168.1602477
		5/2	2.653	73.1		-1.055	-168.1722319
$ReSi_{28}$	C_2	1/2	2.639	30.2	^2B	-0.022	-183.1472281
		3/2	2.717	60.9	^4B	-0.474	-183.1654843
		5/2	2.797	-172.4	^6A	----	-183.0658974
	C_1	1/2	2.661	73.1		-0.802	-183.1725519
		3/2	2.629	77.3		-0.821	-183.1448853
		5/2	2.736	52.6	^6A	-0.009	**-183.1839227**
$ReSi_{32}$	C_1	1/2	2.6402	55.9	^2A	-0.004	**-198.1969785**
		3/2	2.6263	46.1		-0.346	-198.1093921
		5/2	2.7452	38.3		0.374	-198.1951799
$ReSi_{36}$	C_{2v}	1/2	4.097	30.5	$^2B_1$	0.293	-212.8904139
		3/2	3.992	25.9	$^4A_1$	0.231	-212.9400203
	C_1	3/2	3.974	33.8		0.323	-213.052496
	C_1	5/2	3.879	35.8	^6A	0.350	**-213.1788852**
$ReSi_{40}$	C_1	1/2	3.995	30.3		0.324	-228.131402
		3/2	2.598	33.4		0.283	-228.2107318
		5/2	3.836	23.7	^6A	0.333	**-228.2316637**
		7/2	2.564	21.4		0.234	-228.1875406

Si(i) (I=1-16) play an important role in the stability of the $ReSi_{16}$ clusters.

According to the optimized geometry of the quartet C_s isomer, the Re atom deviates to the center site of the Si_{16} frame. In analogy to the doublet $ReSi_{16}$ isomer, the charges transfer mainly from the Si(i) (i=1-8) to the Re atom, the Mullikan atomic net population shows that the Re atom carries −3.438e, which is bigger than that of the doublet $ReSi_{16}$ isomer, reflecting that the electrostatic interactions among the transition metal Re and silicons in the quartet isomer are stronger than in the doublet isomer.

The sextet C_s isomer, which is slightly distorted the C_{4v} isomer, is optimized at the UHF/LanL2DZ level. On the basis of the Figure 1, one finds that the Re atom, which deviates to the center site of the C_{4v} cage, results in the lower-symmetry C_s isomer. The Mullikan atomic net

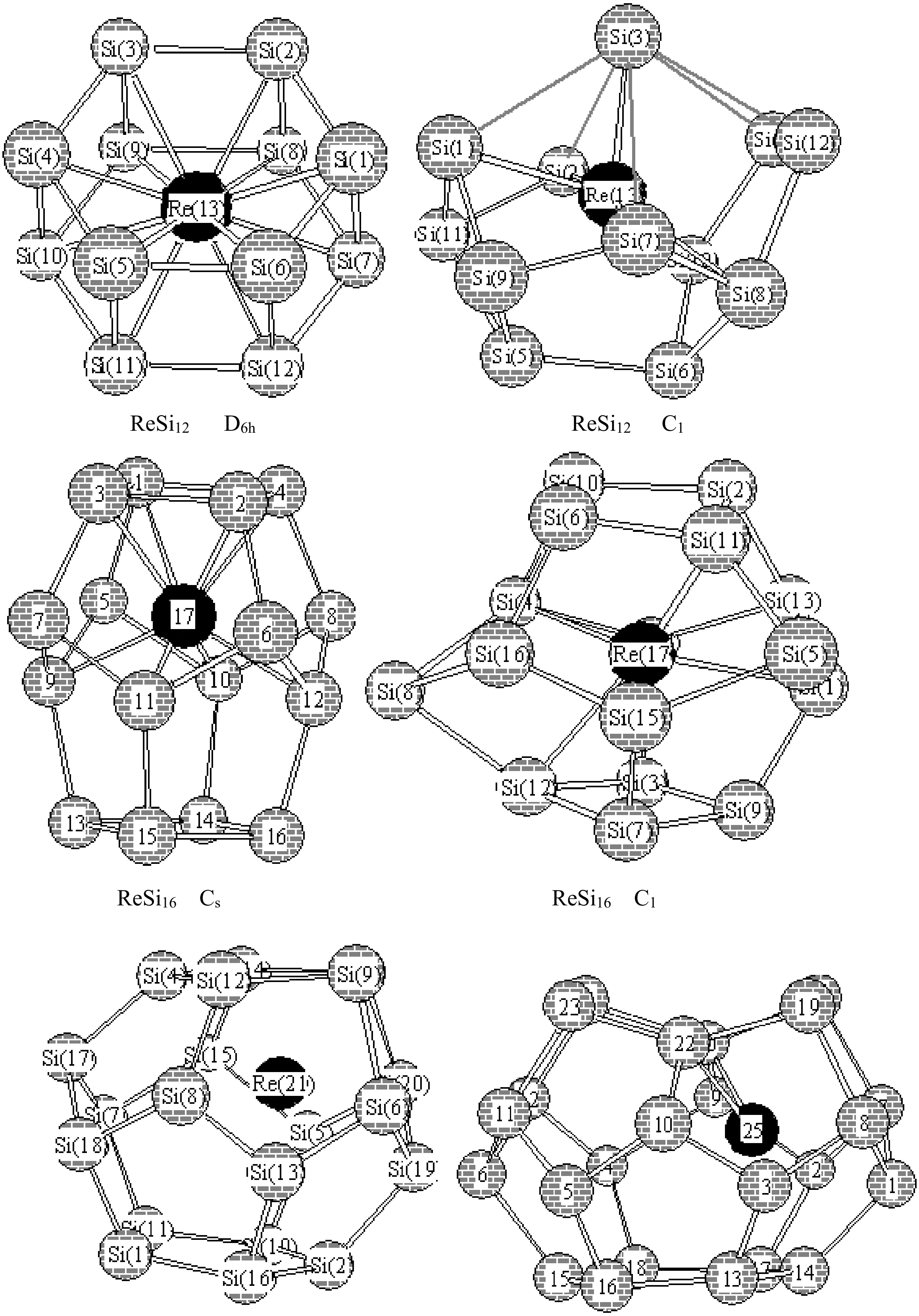

$ReSi_{12}$ D_{6h} $ReSi_{12}$ C_1

$ReSi_{16}$ C_s $ReSi_{16}$ C_1

$ReSi_{20}$ C_1 $ReSi_{24}$ C_1

Figure 1: The stable Re@Sin clusters, where the black atom in the figure represents the Re atom.

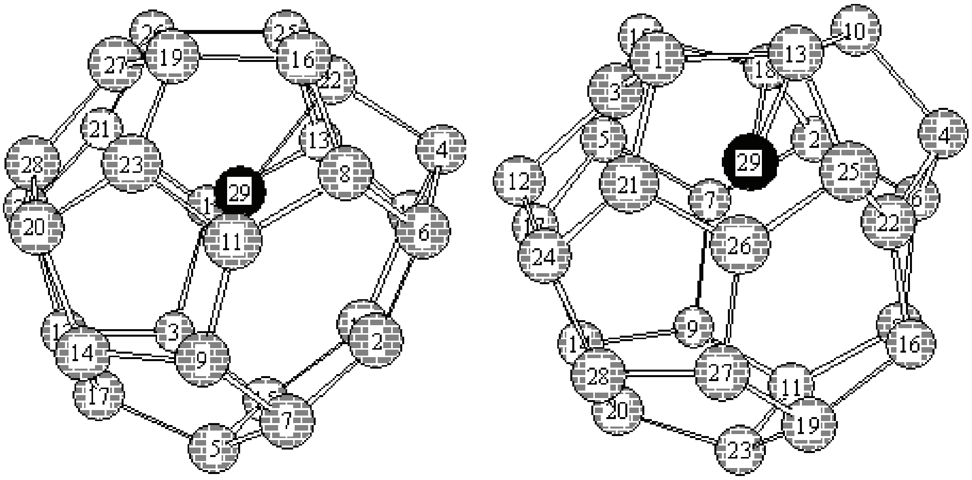

ReSi$_{28}$(a) C$_2$ ReSi$_{28}$ C$_1$

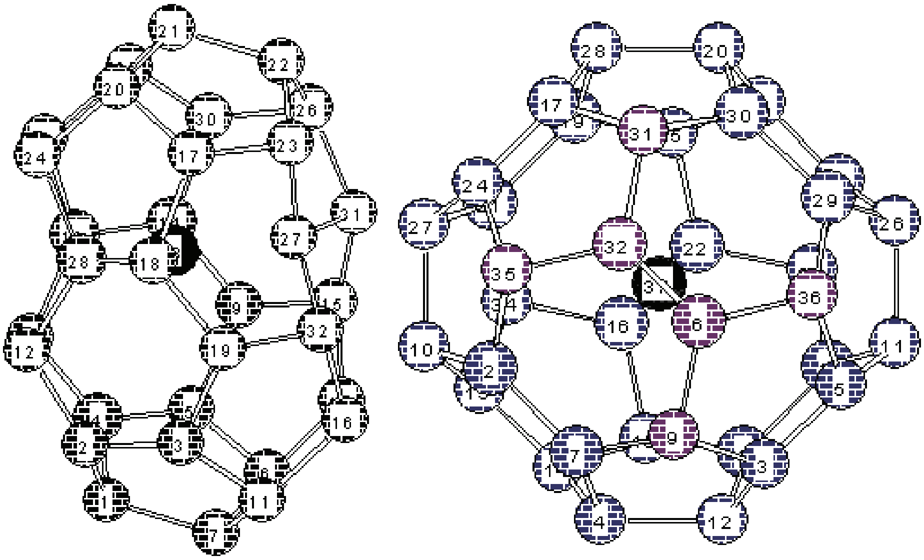

ReSi$_{32}$ C$_1$ ReSi$_{36}$ C$_{2v}$

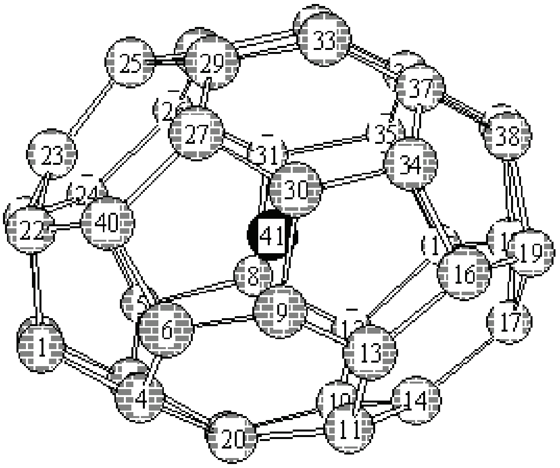

ReSi$_{40}$ C$_1$

Figure 1: (Continued)

population of the Re atom is –3.659e, which is transferred from the Si(i) (i=1-8) atoms.

In addition, the Mullikan atomic net populations of the Re atom in the C_s isomer depend on the spin states, the charge-transformation and the electrostatic interactions among Re and Si_n atoms are increased as spin S goes from S=1/2 to S=5/2. The Re atom tends to saturate the dangling bonds of the Si(i) (i=1-8) atoms; on the other hands, the C_s $ReSi_{16}$ frame with Re atom being localized at the cage center of the Si_{16} frame is less stable than with Re atom being deviated to the cage center of the Si_{16} frame.

According to the optimized equilibrium geometries, it is of interesting that the Si-Si bond lengths of the tetragon rings are longer than those of the pentagonal rings, which are very important for the analysis of the structure criterion of the Si_n fullerene; this finding is similar to that of the carbon fullerene (Buehl and Hirsch, 2001). As can be seen from the total energies of the C_1 and C_s isomers, which are listed in Table 1, they exhibit that the doublet C_s isomer is the lowest-energy structure and the ground state, the electronic state is labeled as having $^2A'$ character.

According to the contour of HOMO orbotals and DOS of the most stable Re and $ReSi_{16}$ nanocages (Figure 2), it is easy to find that Re atom forms chemical bonds with surrounding Si atoms after Re atom is encapsulated Si_{16} cage and the DOS near HOMO orbitals is increased.

2.3 $ReSi_{20}$

The possible $ReSi_{20}$ cages are investigated. The three distinct isomers with D_{2d}, C_{2v}, and C_2 symmetries are optimized with several imaginary frequencies having been found. After the $ReSi_{20}$ cage exhibiting maximum symmetry undergoes slightly distortions into more stable structure with low symmetry, the stable doublet C_1 isomer is generated.

By distorting the geometry from the D_{2d} isomer, the newer doublet C_1 $ReSi_{20}$ isomer is yielded. Theoretical results show that the encapsulated Re atom in the $ReSi_{20}$ cage deviates the cage center of the slight distorted D_5d Si_{20} frame and prefers to interacting with Si(3) and Si(6) atoms with the shortest Re-Si(3) and Re-Si(6) bond lengths

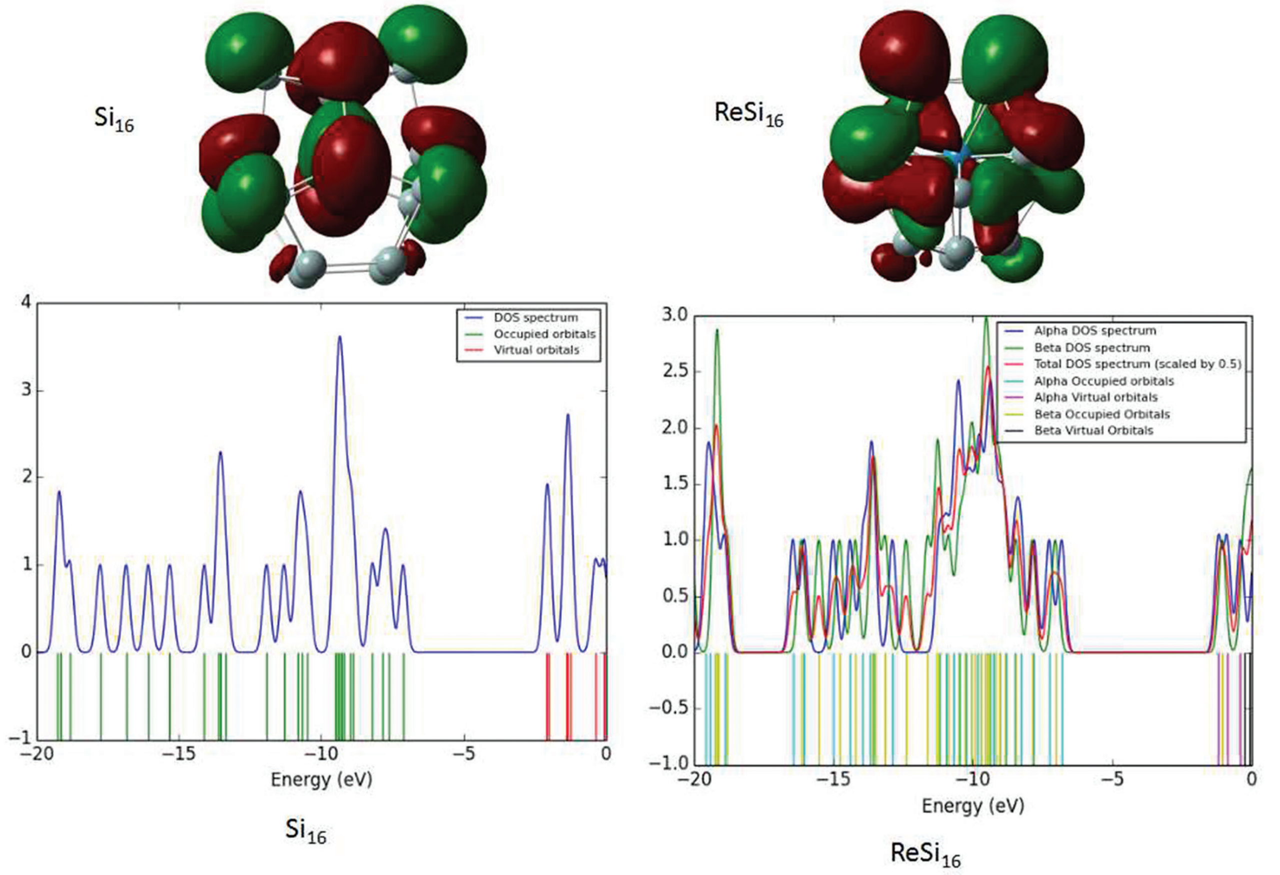

Figure 2: DOS and contours of HOMO orbitals of respective Si_{16} and $ReSi_{16}$ nanocages.

of 2.710 Å. The Mullikan atomic net population of the Re atom in the C_1 isomer carries –1.764e, which transfers mainly from the Si(i) (i=3, 6, 9, 12, 15, 16, 19, and 20) atoms.

The Re atom in the stable quartet C_1 $ReSi_{20}$ cluster moves to the most favored adsorption site of the inner surface of the Si(6) atom with the shortest Re-Si(6) bond length of 2.744 Å; the Mullikan atomic net population of the Re in the quartet C_1 isomer is –2.145e, the obtained charges of the Re atom come mainly from the Si(3), Si(6), and Si(9) atoms.

As far as the sextet C_1 isomer is concerned, the final optimized geometry exhibits that the Re atom deviates to the cage center site of the Si_{20} frame, and that the Re is bound to the inner surface of the Si(6) atom with the shortest Re-Si(6) of 2.725 Å. On the ground of equilibrium geometry, it apparently shows that the doped Re atom results in the significant distortion of the Si_{20} geometry as well as the charge distributions. The Re atom carries –2.147e, the charges mainly come from the Si(3), Si(6), Si(9), and Si(12) atoms with Mullikan charges being 0.348, 0.288, 0.417, and 0.305e, respectively.

As can be seen from the calculated Mullikan charges of the Re atom and total energy of the $ReSi_{20}$ unit, the Mullikan net populations of the Re atom depend on the spin states. Furthermore, the doublet $ReSi_{20}$ isomer is the most stable isomer.

2.4 $ReSi_{24}$

The optimized geometries indicate that the possible $ReSi_{24}$ isomers with high symmetries are not the stable geometries. However, after undergoing the slight distortion of the $ReSi_{24}$ geometry to the low symmetry, the stable C_1 isomer is obtained finally. Furthermore, the stable C_1 $ReSi_{24}$ geometry slightly distorts the initial geometry with the transitional metal Re being localized at the cage center of the Si_{24} frame. Specifically, this geometry, which composes of 12 Si_5 rings and 2 Si_6 rings, is analogous to that of the C_{24} fullerene. The calculated results show that the geometry is deformed because of the interactions between the Si_{24} frame and Re, furthermore, the distortion of the Si_{24} frame depends on the selected binding site of the Re atom.

It is found that the slight distorted doublet $ReSi_{24}$ frame with Re atom being localized at the center site of cage is not the most stable isomer. The Re atom in the $ReSi_{24}$ frame favors attached the inner surface site of the Si_{24} fullerene and moves from the cage center of the Si_{24} frame to the inner surface site that is near the Si(22) and Si(20) atoms with the shortest Re-Si bond lengths of 2.63 Å, this phenomenon indicates that the electrostatic interactions among the Re atom and the Si(20) or Si(22) atom lead to the sinking of the Si(20) and Si(22) atoms into the surface of the Si_{24} frame. The Mullikan atomic net population of the Re, Si(19), and Si(24) atoms are –1.530, 0.309, and 0.294e, respectively; The obtained charge of Re atom is transferred mainly from the Si(1), S(8), Si(10), Si(19), and Si(24) atoms. According to the calculated Mullikan atomic net populations, it shows that the Re atom in the doublet $ReSi_{24}$ fullerene acts as an acceptor of the charges and tries to terminate the dangling bonds of the Si(20) and Si(22) atoms. The electrostatic interactions among the Re and Si_n atoms alter the charge distributions and fullerene geometry of the Si_{24} frame as well as the stability of the $ReSi_{24}$ frame.

The Re atom in the quartet $ReSi_{24}$ fullerene moves from the cage center site to the inner surfaces of the Si(18) and Si(23) atoms with the shortest Re-Si(18) and Re-Si(23) bond lengths being respective 2.678 and 2.660 Å; Furthermore, the Si(18) and Si(23) atoms have the tendency to sink from the surface of the Si_{24} frame because of the electrostatic interactions of the Re atom and Si(20) or Si(23) atoms. Consequently, the Si_{24} geometry is distinctly distorted after the Re atom is encapsulated into the Si_{24} frame. Mullikan atomic net population of the Re atom in the quartet $ReSi_{24}$ isomer is −0.206e, which is smaller than that of the doublet isomer, indicating that charge-transfer among the Re and Si_{24} frame of the quartet $ReSi_{24}$ isomer is smaller than that of the double isomer, in other words, the electrostatic interactions between the Re and Si_{24} frame in the quartet isomer are weakened as compared to the doublet isomer, therefore, the Re atom in the quartet $ReSi_{24}$ fullerene makes a less contribution to the stability than that of the doublet isomer. Consequently, the doublet $ReSi_{24}$ fullerene is more stable than that of the quartet isomer. These findings can be certified by the calculated total energies.

The sextet $ReSi_{24}$ cage is taken into account, the Re atom in the $ReSi_{24}$ cage moves from the cage center site to the inner surface site of an adjacent Si(6), Si(14), and Si(19) atoms with the shorter Si(6)-Re, Si(14)-Re, and Si(19)-Re bond lengths being respective 2.653, 2.852, and 2.855 Å. The electrostatic interactions between the Re and Si(i) (i=6, 14, and 19) atoms, which result in the distorted geometry, are stronger than those of the others; the main populations of the Si(8), Si(13), Si(14), Si(17), and Si(23) atoms are 0.244, 0.314, 0.259, −0.210, and −0.165 e, respectively; the atomic net population of the Re atom in the $ReSi_{24}$ cage is –1.055e, indicating that the Re atom obtains the charges from its neighbor Si atoms.

According to the optimized equilibrium geometries of the doublet, quartet, and sextet $ReSi_{24}$ cages, one should be noticed that the Re atom in the $ReSi_{24}$ cage deviates to the initial cage center of the Si_{24} frame. Furthermore, the total energy of the doublet $ReSi_{24}$ cage is the lowest one, indicating that the doublet $ReSi_{24}$ cage is the most stable structure.

2.5 $ReSi_{28}$

The novel molecular and electronic structures associated with endohedral metallofullerenes have attracted attentions (Turker, 2001a; Turker, 2001b). The initial geometry of the D_{2h} $ReSi_{28}$ fullerene with the Re atom being inserted in the cage center of the Si_{28} cage are optimized at the UHF level. According to the calculated results, which summarizes at the Table 1 and Figure 1, one finds that the Re atom in the essential final geometry deviates to the cage center of the Si_{28} frame, indicating that the $ReSi_{28}$ frame with higher symmetry undergoes the distortion of the geometry into the much more stable structure with lower C_2 symmetry, reflecting that the doublet C_2 $ReSi_{28}$ fullerene with the Re atom localized at the cage center is higher in total energy than that with the Re atom being localized at the site, which is near the Si(1) and Si(22) atoms. The Mulliken atomic net population of the Re atom is very small, namely, −0.022e. In other words, the charge-transfer among the Re atom and Si_{28} fullerene is small, the electrostatic interactions among the transition metal Re and the Si_{28} fullerene are weakened. However, the doped Re atom contributes to the charge distribution of the Si_{28} fullerene. The Si(1) atom obtains more charges from the Si(3), Si(13), and Si(23) atoms; and the Si(22) atom obtains mainly charges from the Si(4), Si(16), and Si(25) atoms.

The Re atom of the quartet C_2 $ReSi_{28}$ cage moves to the inner surface site near the Si(1) and Si(22) atoms, the movement of the Re atom finally results in the distortion of the Si_{28} cage and the sinking of the Si(1) and Si(22) atom to the inner Si_{28} surface. Furthermore, the Si-Si bond lengths and charge distributions are changed after the Re atom is encapsulated into Si_{28} frame; this phenomenon is similar to that of the doublet isomer. The Re atom of the quartet isomer carries −0.474e, which is bigger than the doublet isomer and is transferred mainly from the Si(13) and Si(25) atoms with population of 0.357 e, in other words, the electrostatic interactions between the Re atom and Si frame for the quartet isomer are stronger than that of the doublet isomer. Consequently, the electrostatic interactions between Si(1) or Si(22) atom and Re atom in the quartet isomer enhance the stabilities of the $ReSi_{28}$ cluster. As for the sextet C_2 $ReSi_{28}$ isomer, the frequency analysis proves that the C_2 $ReSi_{28}$ is a transition state. On the ground of the calculated total energies of the C_2 isomers, it exhibits that the quartet C_2 isomer is more stable than the doublet isomer.

The doublet C_1 isomer is calculated. Specifically, this geometry is seriously distorted the C_2 isomer mentioned above. The Re atom has a strong interaction with Si(18) atom, and the attractive interactions cause the seriously deviation of the Si_{28} surface. The Mullikan atomic net population of the Re atom is −0.802e, which is bigger than that of C_2 isomer, in other words, the electrostatic interaction of the C_1 isomer is stronger than those of the C_2 isomer. As a consequence, the Si_{28} fame distorted more seriously. Additionally, the charges of the Si_{28} surface are redistributed.

As for the quartet C_1 isomer. The calculated results show that the Re atom in the cage is shifted toward the inner surface site, which are near Si(13) and Si(18) atoms. The Mullikan net population of the Re atom is −0.821 e. The Re atom in the $ReSi_{28}$ frame behaviors as an acceptor of charges, because the unsaturated 5d orbitals of Re atom interests to pull more charges from Si atoms. The electrostatic interactions among the Re and Si_n frame enhance the stability of the quartet $ReSi_{28}$ cage.

For the sextet C_1 $ReSi_{28}$ cage, the Re atom selects the Si(26) atom as the binding site in the sextet C_1 $ReSi_{28}$ cage with the shortest Si(26)-Re bond length being 2.736 Å, resulting in the adjustments and alternations of the locations of the Si frame. As a consequence, the electronic properties and bond lengths of the Si_{28} frame are influenced slightly by the rearrangement of the Si_{28} geometry. Especially, the Si_n atoms, which connect the binding site of Re atom, are adjusted slightly under the attractive interactions of the Re atom and charge redistributions. The Mullikan atom net population of the Re atom is −0.009e, reflecting that charge-transfer among the Re and Si_{28} fullerene is very small. In the C_1 $ReSi_{28}$ cage, the charges mainly transfer from Si(15) (0.252e) and Si(25) (0.288e) atoms to Si(18) (−0.308e) and Si(26) (−0.354e) atoms.

Inspection of the calculated total energies of the C_1 and C_2 $ReSi_{28}$ cages (Table 1), the sextet C_1 isomer is about 0.309 eV lower in total energy than the doublet C_1 isomer, thus, the sextet C_1 isomer corresponds to the ground state. On the basis of the calculated equilibrium geometry and Mullikan atomic net population of the Re atom in the sextet C_1 isomer, one finds that the shortest Re-Si(26) bond length in the sextet C_1 isomer is longer than those of the most stable $ReSi_n$ (n=1-12, 16, 20, 24) clusters and the charge-transformation among Re and Si_n frame in the sextet C_1 isomer is very small, therefore, the electrostatic interaction of the Re and C_1 Si_{28} frame makes a little influence to the inserted Re atom, consequently, the inserted Re atom in the sextet isomer keeps the same electronic state as the free septet Re atom.

2.6 $ReSi_{32}$

The equilibrium geometry of the doublet C_1 $ReSi_{32}$ cage, which is composed of 14 Si_5 rings and 4 Si_6 rings, is optimized. According to the calculated results, it exhibits that the doped Re atom has a tendency to move from the cage center toward the inner surface site of the Si(28) atom. This finding indicates that the geometry with Re atom being localized at the cage center of the Si_{32} frame is higher in total energy than with Re atom being localized at the inner surface of the Si(28) atom. The Mullikan net populations of the Si(27) and Si(28) atoms are −0.231e and −0.207e, respectively. It is worthwhile pointing out that the negative charges are mainly localized at the concaved Si(27) and Si(28) atoms. The net population of the Re atom (−0.004) is negative, and the charges are transferred to the Si(5) atom, the electrostatic interaction between the Si(28) and Re is weaker. Therefore, the doped-Re atom plays a little bit contribution in the slight distorted geometry.

The calculated geometry shows that the Re atom is shifted toward the inner surface of the Si(28) atom. Furthermore, the Mullikan atomic net population of the Re atom in the $ReSi_{32}$ cage is −0.346e, which is bigger than the doublet C_1 $ReSi_{32}$ geometry; one concludes that the interactions among the Re and Si_{32} frame in the quartet isomer are stronger than those of the doublet isomer, and their influences to the Re atom and the Si_{32} frame are stronger. The quartet C_1 structure undergoes the slight deviation in geometry and forms the stable geometry because of the electrostatic interactions of the encapsulated Re atom.

As can be seen from the findings related to the geometries of the examined systems, the Re atom in the Si_{32} frame is localized at the inner surface site of the Si(8) and Si(27) atoms with the Re-Si(8) and Re-Si(27) distances being respective 2.745 and 2.804 Å. The Mullikan atomic net population of Re atom is 0.374 e; indicating that the charges are transferred from the Re atom to the Si_{32} frame. According to the Mullikan atomic spin populations, the magnetism is predicted as 5.0 Bohr magnets, which are dominantly contributed from the Re atom.

In general, Re atom reduces the distortion of the Si_{32} frame. The calculated total energies show that the doublet $ReSi_{32}$ cage is the lowest-energy structure and ground state. Based upon the contour of HOMO orbitals and DOS of respective Si_{32} and $ReSi_{32}$ nanocages, we can find that Re atom interacts with Si atoms with σ bonding after Re atom is encapsulated into Si_{32} cage (Figure 3). Furthermore, the DOS near HOMO or LUMO orbitals for $ReSi_{32}$ is increased as compared with that of Si_{32}. Thus, the encapsulated Re atom makes great contribution to stable silicon frame.

2.7 $ReSi_{36}$

On the basis of the initial geometry of the D_{2d} Si_{36} cage at the AM1 level (Han et al., 2003), the C_{2v} $ReSi_{36}$ cluster with Re atom being encapsulated in the cage center of Si_{36} fullerene is optimized. The calculated harmonic vibrational frequency analysis reveals that the C_{2v} $ReSi_{36}$ (S= 1/2 and 3/2) cages are the stable structures. Specifically, the encapsulated Re atom localizes at the cage center and tries to interact with all Si atoms simultaneously with the weak electrostatic interactions.

As far as the doublet $ReSi_{36}$ cage is concerned. The Mullikan atomic populations of the Re atom in the doublet and quartet isomers is 0.293 and 0.231e, therefore, the Re acts as the donor of the charge, the doublet isomer contributes less charge to the Si_{36} cage than that of the doublet form. Unfortunately, the sextet C_{2v} isomer turns out to be unstable geometries. After the distortion of the C_{2v} geometry, the stable C_1 isomer is born. For the quartet and sextet C_1 $ReSi_{36}$ cages, the Re atom at the quartet and sextet isomer locates at off-center position of the Si_{36} cage with the shortest Re-Si(6) and Re-Si(32) bond lengths of 3.974 and 3.879 Å, respectively. The Re in the quartet and sextet isomers carries 0.323 and 0.350e, respectively.

On the basis of the calculated total energies which are listed in Table 1, it indicates that the sextet C_1 isomer is the lowest-energy isomer.

2.8 $ReSi_{40}$

Initial geometry of D_{5d} $ReSi_{40}$ cage with the encapsulated Re atom being localized at the cage center is considered; However, the calculated results prove that there are several imaginary frequencies and the corresponding geometries are turned out not to be the stable structures. After the $ReSi_{40}$ cage of maximum symmetry undergoes a slight distortion into much more stable structure of lower symmetry, the most stable cage corresponds to the lower symmetry.

Inspection of the data in Table 1 and Figure 1, it obviously shows that the Re atom deviates the cage center of the Si_{40} frame and moves toward to the inner

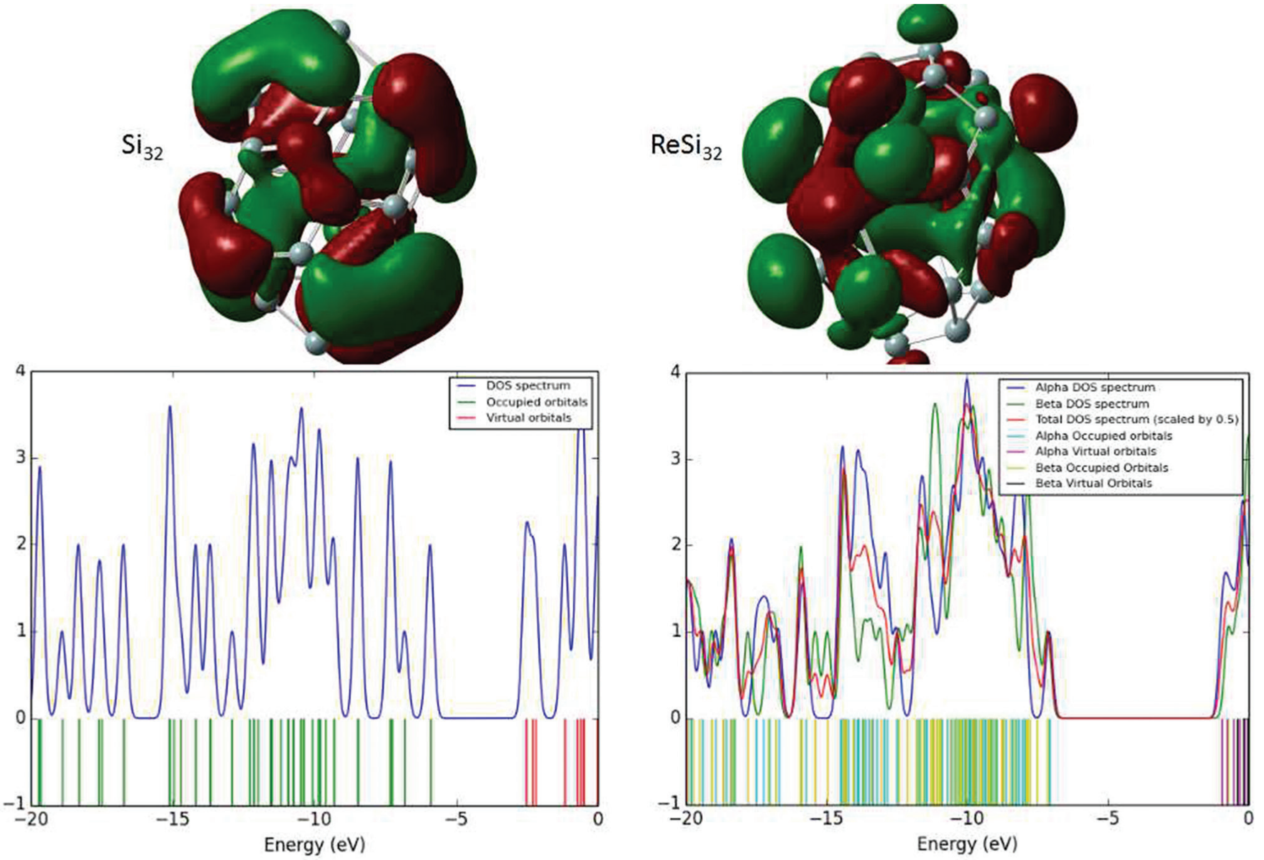

Si_{32} $ReSi_{32}$

Figure 3: DOS and contours of HOMO orbitals of respective Si_{32} and $ReSi_{32}$ nanocages.

surface of the Si(20) atom, along with the distortion of the Si_{40} cage. In other words, the final spheroidal geometry is disturbed nearby the dopant Re atom. The Re atom carries 0.324e, the charges are mainly shifted out of the Re atom to the Si(20) atom and its neighbors, reflecting that the Re atom acts as donor, and that the charge-transfer between the encapsulated Re atom and Si_{40} fullerene is very small, the electrostatic interactions among the Re atom and Si_{40} fullerene are weak. The charge-transfer of the Si_{40} frame is small, indicating that the Si-Si covalent bonds play the fundamental role in the cage stabilities.

The calculated results on the quartet isomer show that the equilibrium geometry is distorted in the presence of the encapsulated Re atom and the encapsulated Re atom moves to the inner surface of the Si(33) atom. Mullikan atomic population of the encapsulated Re atom is 0.283e, exhibiting that the charges are transferred from the Re atom to the neighboring Si atoms.

For sextet isomer, the shortest Re-Si(10) bond length is predicted to be 3.836 Å, reflecting that the encapsulated Re atom deviates the cage center site of the $ReSi_{40}$ frame and moves toward to the Si(10) atom, together with the slight distortion of the Si_{40} frame. The populations of the encapsulated Re atom and the Si(10) atom are respective 0.333e and −0.229e, indicating that the electrostatic interactions among the Re atom and Si_{40} frame are weakened, and that the charges are transferred from the Si(10) atom to the Re atom. The biggest positive charge in the Si_{40} frame is localized at the Si(7) atom (0.161e).

The equilibrium geometry of the octet C_1 $ReSi_{40}$ isomer is analogous to that of the quartet isomer. On the basis of the calculated total energies of the $ReSi_{40}$ isomer with spin S=1/2, 3/2, 5/2, and 7/2, the octet isomer is lower in total energy than the quartet isomer. Furthermore, the sextet isomer is the lowest-energy isomer, which is selected to be a ground state.

3 Relative stability

In order to discuss the relative stabilities of the $ReSi_n$(n=16, 20, 24, 28, 32, 36, and 40) cages, the dissociation energies with respect to the removal of the Si_4 and Si units as well as the atomic averaged bind energies are calculated according to the following formula:

$$D(n,n\text{-}4) = E_T(Si_4) + E_T(ReSi_{n\text{-}4}) - E_T(ReSi_n)$$

$$A(n)= [4\ E_T(Si) + E_T(ReSi_{n\text{-}4}) - E_T(ReSi_n)]/4$$

Where $E_T(Si_4)$, $E_T(Si)$, $E_T(Re)$, and $E_T(ReSi_n)$ represent the total energies of the most stable Si_4, Si, Re, and $ReSi_n$ clusters, respectively. On the basis of the calculated results listed at Table 2 and shown in Figure 4, it manifests that the calclated D(n,n-4) results exhibit the same variable tendency as A(n) results in Figure 4, reflecting that the calculated fragmentation energies of D(n,n-4) and A(n) of the investigated clusters are stable with respect to the dissociation into Si_n atoms and give the reasonable explanations of the relative stabilities of the $ReSi_n$ clusters. The calculated fragmentation energies for the $ReSi_n$ clusters exhibit that the D(n,n-4) and A(n) increase as the n goes from n=20 to n=40, two peaks are found at n=16 and 40, which correspond to the stable magic numbers. Because D(40,36) is slightly smaller than D(16,12), and the remarkable D(16,12) and A(16) values are found, consequently, n=16 corresponds to the magic number of stability. This finding shows that the $ReSi_{16}$ is the most stable isomer and is similar to theoretical predictions on stable magic numbers of $PtSi_n$ and $PdSi_n$ clusters (Han et al., 2007; Wang and Han, 2005b; Zhao et al., 2014).

4 Computational details

In order to compare with available theoretical results and to test the reliability of the theoretical approach for the $ReSi_n$ (n=12, 16, 20, 24, 28, 32, 36, and 40) cages, the ReSi and Si_2 dimers are calculated at the HF/LanL2DZ level, the calculated Re-Si and Si-Si bond lengths of the most stable quartet ReSi and triplet Si_2 isomers are respective 2.595 and 2.520 Å; the Re-Si bond length of the ReSi dimer at the HF/LanL2DZ level is slightly longer than at the UB3LYP/LanL2DZ level (Han and Shi, 2001). The possible geometries of the $ReSi_n$ (n=12, 16, 20, 24, 28, 32, 36, and 40) cages are considered and carried out at the UHF/LanL2DZ level by using of Gaussian 98 program (Frisch et al., 1998). For each stationary point of the cages, the stability is examined by the harmonic vibrational frequency. For cases existing an imaginary frequency, a relaxation along the coordination of the imaginary vibrational mode is performed until the true minimum is reached. Therefore, the geometries for each cage and its isomers are the stable structures, which correspond to the local minima. The fragmentation energies with respect to the remove of the Si_4 and Si units are obtained as the criterion of discussing relative stability of the $ReSi_n$ cages.

5 Conclusions

Systems of the form Re@Si_n (n=12, 16, 20, 24, 28, 32, 36, 40) with different spin states were studied at the UHF/LanL2DZ level. In this work, equilibrium geometries, total energies, stabilities, and Mullikan atomic net populations of the Re atom in Re@Si_n clusters were examined. The results demonstrate that all $ReSi_n$ systems with initial higher symmetric structures undergo slight distortions into geometries of sizeable higher stability with lower symmetry. The Re atom in Re@Si_n (n=12, 16, 20, 24, 28, 32, 36, and 40) cages locates at off-center positions of Si_n clusters. Correspondingly, an ionic admixture to the bonding between the Re impurity and the Si cage atoms contributes to the stability of Si_n cages. Furthermore, Mullikan atomic net populations indicate that the charges of Re atom vary gradually from negative to positive as the size of the Si_n cage goes from n=12 to n=40. According to the calculated fragmentation energy, the relative stability of the $ReSi_n$ cages is discussed, and showing that the $ReSi_{16}$ cage is the most stable isomer and the n=16 is seen as the magic number of stability, this finding is similar to the available theoretical results (Wang and Han, 2005b; Zhao et al., 2014).

Acknowledgments: This work is supported by Physical electronics disciplines (NO: 12XKJC01). This paper has been performed on the Supercomputer Center of University of Science and Technology of China.

Table 2: The calculated fragmentation energies (D(n,n-4)) and averaged **atomic** binding energies (A(n)) of the most stable Re@Si_n clusters(units: eV).

n	12	16	20	24	28	32	36	40
D(n,n-4)	3.973	5.948	3.768	4.350	4.540	4.598	3.750	5.679
A(n)	7.819	9.794	7.614	8.196	8.386	8.444	7.596	9.525

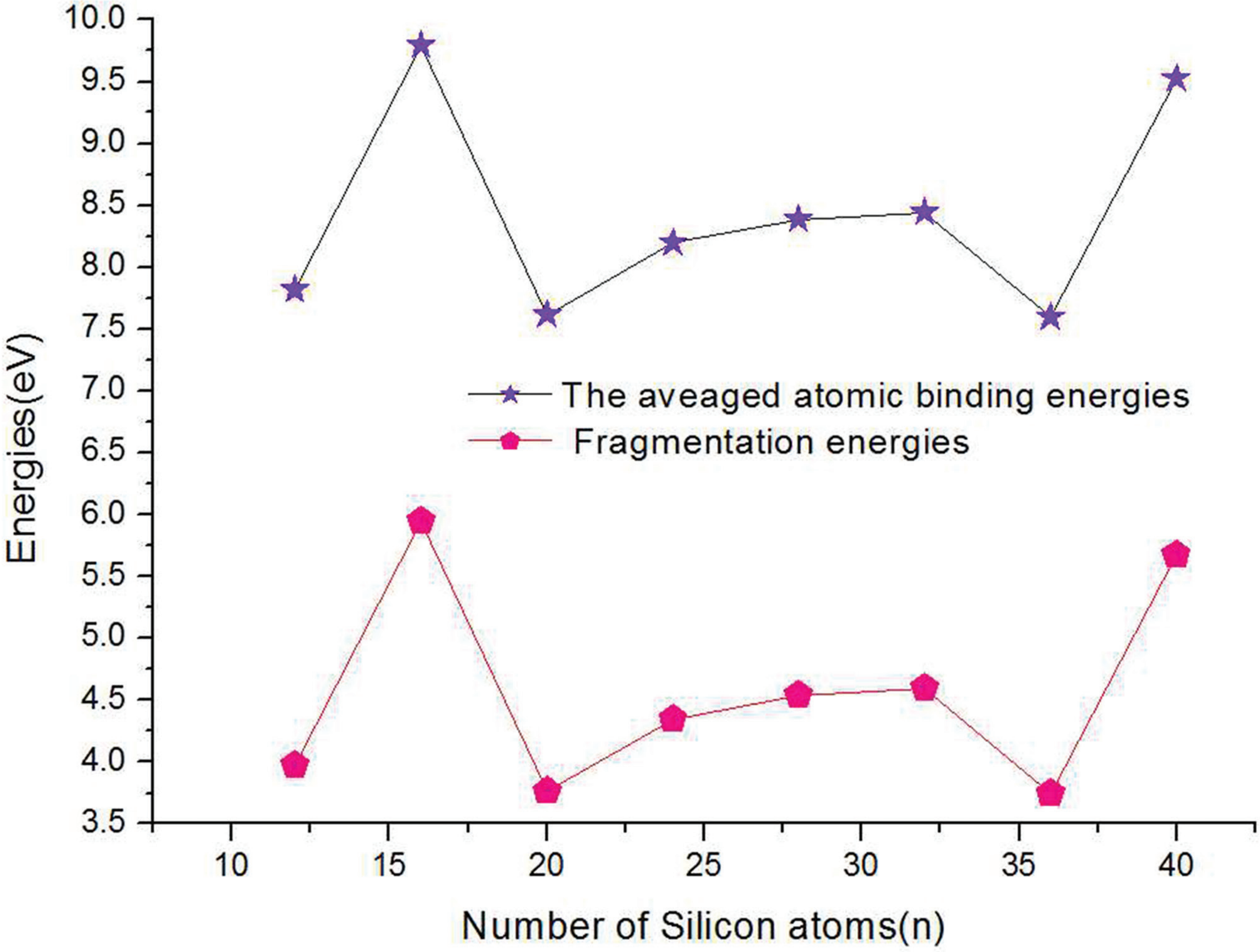

Figure 4: The calculated averaged atomic binding energies and fragmentation energies of Re doped silicon cages.

References

Buehl M., Hirsch A., Spherical aromaticity of fullerenes. Chem. Rev., 2001, 101, 1153-1183.

Chen R., Lin F., Jin H., Zhao R.N., Geometrical and Electronic Properties of $PdWSi_n$ (n=10-20) Semiconductor materials. Main Group Met. Chem., 2018, 41, 33-41.

Frisch M.J., Trucks G.W., Schlegel H.B., Scuseria G.E., Robb M.A., Cheeseman J.R., et al., Gaussian 98. Gaussian, Inc., Pittsburgh PA, 1998.

Hiura H., Miyazaki T., Kanayama T., Formation of metal-encapsulating Si cage clusters. Phys. Rev. Lett., 2001, 86, 1733-1736.

Jarrold M.F., Nanosurface chemistry on size-selected silicon clusters. Science, 1991, 251, 1085-1092.

Jackson K., Nellermoe B., Zr@Si20: a strongly bound Si endohedral system. Chem. Phys. Lett., 1996, 254,249-256.

Guo P., Yang A.P., Ren Z.Y., Han J.G., Bian J., Wang G.H., A Relativistic Computational Investigation: the Electronic Structures and Properties of $TaSi_n^+$ (n=1-13, 16) Clusters. J. Phys. Chem. A, 2006, 110, 7453-7460.

Han J.G., Shi Y.Y., A computational study on geometries, electronic structures and Ionization potentials of MSi_{15} (M=Cr,Mo,W) clusters by density functional method. Chem. Phys., 2001, 266, 33-40.

Han J.G., Xiao X., Hagelberg F., Geometry and electronic structure of WSi_n (n=1-6,12) clusters. Struct. Chem., 2002, 13, 173-191.

Han J.G., A theoretical investigation on electronic properties and stability of $IrSi_x$(x=1-6) clusters. Chem. Phys., 2003, 286, 181-192.

Han J.G., Ren Z.Y., Sheng L.S., Zhang Y.W., Morales J.A., Hagelberg F., The formation of new silicon cages: a semiempirical theoretical investigation. J. Mol. Struct. (THEOCHEM), 2003, 625, 47-58.

Han J.G., Ren Z.Y., Lu B.Z.,Geometries and stabilities of Re-doped Si_n (n=1-12) clusters: A DFT investigation. J. Phys. Chem. A, 2004, 108, 5100-5110.

Han J.G., Zhao R.N., Duan Y.H., The growth patterns and electronic properties of the cagelike Mo_2 doped-Si_x (x=9-16) clusters. J. Phys. Chem. A, 2007, 111, 2148-2155.

Han J.G., Hagelberg F., Recent Progress in the Computational Study of Silicon and Germanium Clusters with Transition Metal Impurities. J. Comput. Theor. Nanosci., 2009, 6, 257-269.

Majumder C., Kulshreshtha S.K., Impurity-doped Si_{10} cluster: Understanding the structural and electronic properties from first-principles calculations. Phys. Rev. B, 2004, 70, 245426.

Miyazaki T., Hiura H., Kanayama T., Topology and energetic of metal-encapsulating Si fullerenelike cage clusters. Phys. Rev. B, 2002, 66, 121403.

Piqueras M.C., Crepo R., Orti E., Tomas F., AM1 Prediction of Equilibrium Geometry of Si_{60}. Chem. Phys. Lett., 1993, 213, 509-513.

Shvartsburg A.A., Liu B., Jarrold M.F., Ho K.M., Modeling ionic mobilities by scattering on electronic density isosurfaces: Application to silicon cluster anions. J. Chem. Phys., 2000, 112, 4517-4526.

Turker L., Theoretical aspects of Si_{60} structure having endohedral beryllium species, Be and Be^{+2}. J. Mol. Struct. (THEOCHEM), 2001a, 548, 185-189.

Turker L., Endohedrally palladium doped Si-60-ZINDO/1 treatment. J. Mol. Struct. (THEOCHEM), 2001b, 546, 45-49.

Wang J., Han J.G., A computational Investigation on Germanium and Copper-doped Germanium clusters by the density functional method. J. Chem. Phys., 2005a, 123, 244303.

Wang J., Han J.G., Geometries, Stabilities and Electronic properties of different sized $ZrSi_n$ (n=1-16) clusters: A density functional investigation. J. Chem. Phys., 2005b, 123, 064306.

Wang J., Han J.G., A theoretical study on the growth patterns: The Ni-doped germanium clusters. J. Phys. Chem. B, 2006, 110, 7820-7827.

Wu J.H., Hagelberg F., Equilibrium geometries and associated energetic properties of mixed metal- silicon clusters from global optimization. J. Phys. Chem. A, 2009, 110, 5901-5908.

Xiao C., Hageberg F., Lester W.A., Geometric, energetic, and bonding properties of neutral and charged copper-doped silicon clusters. Phys. Rev. B, 2002, 66, 075425.

Xu H.G., Zhang Z.G., Feng Y.A., Zheng W.J., Photoelectron spectroscopy and density-functional study of $Sc_2Si_n^-$ (n = 2–6) clusters. Chem. Phys. Lett., 2010, 498, 22-36.

Yang J.C., Wang J., Hao Y.R., Europium-doped silicon clusters EuSin (n=3-11) and their anions: structures, thermochemistry, electron affinities, and magnetic moments. Theor. Chem. Acc., 2015, 134, 81.

Zhao R.N., Han J.G., Duan Y.H., Density Functional Investigation on the Geometrical and Electronic Properties and Growth Patterns of Si_n (n=10-20) Clusters with Bimetal Pd_2 Impurities. Thin Solid Films, 2014, 556, 571-579.

Zhao R.N., Lu Z.C., Han J.G., Geometrical and Electronic Properties of Nanosize Si_m (m=36-90) Clusters with Polymetal Pd_n(n=6-15) Impurities: A Density Functional Theory Investigation. Sci. Adv. Mater., 2016, 8, 2216-2222.

Zhao R.N., Chen R., Yuan Y.H., Han J.G., Duan Y.H., Computational investigation on the structures and electronic properties of the nanosized Rhenium clusters. Solid State Ionics, 2017a, 310, 24-29.

Zhao R.N., Chen R., Liu Z.C., Han J.G., Geometrical and Electronic Properties of Nanosize Semiconductor Pt_2Si_n (n=10-20) material: A Density Functional Theory Investigation. Mater. Sci. Eng. B, 2017b, 226, 151-157.

Zhao R.N., Han J.G., Duan Y.H., A density functional prediction of geometries and stabilities and electronic properties of nanosize cagelike $(InN)_{2n}$ (n=6-27,45,54) semiconductor material. Adv. Theory Simul., 2018, 1, 1800001.